The Cerebellum (2023) 22:261–271
https://doi.org/10.1007/s12311-022-01385-5

ORIGINAL ARTICLE

Real-life Wrist Movement Patterns Capture Motor Impairment in Individuals with Ataxia-Telangiectasia

Anoopum S. Gupta[1] · Anna C. Luddy[1] · Nergis C. Khan[1,2] · Sara Reiling[3] · Jennifer Karlin Thornton[3]

Accepted: 21 February 2022 / Published online: 16 March 2022

Abstract

Sensitive motor outcome measures are needed to efficiently evaluate novel therapies for neurodegenerative diseases. Devices that can passively collect movement data in the home setting can provide continuous and ecologically valid measures of motor function. We tested the hypothesis that movement patterns extracted from continuous wrist accelerometer data capture motor impairment and disease progression in ataxia-telangiectasia. One week of continuous wrist accelerometer data were collected from 31 individuals with ataxia-telangiectasia and 27 controls aged 2–20 years old. Longitudinal wrist sensor data were collected in 14 ataxia-telangiectasia participants and 13 controls. A novel algorithm was developed to extract wrist *submovements* from the velocity time series. Wrist sensor features were compared with caregiver-reported motor function on the Caregiver Priorities and Child Health Index of Life with Disabilities survey and ataxia severity on the neurologist-performed Brief Ataxia Rating Scale. Submovements became smaller, slower, and less variable in ataxia-telangiectasia compared to controls. High-frequency oscillations in submovements were increased, and more variable and low-frequency oscillations were decreased and less variable in ataxia-telangiectasia. Wrist movement features correlated strongly with ataxia severity and caregiver-reported function, demonstrated high reliability, and showed significant progression over a 1-year interval. These results show that passive wrist sensor data produces interpretable and reliable measures that are sensitive to disease change, supporting their potential as ecologically valid motor biomarkers. The ability to obtain these measures from a low-cost sensor that is ubiquitous in smartwatches could help facilitate neurological care and participation in research regardless of geography and socioeconomic status.

Keywords Ataxia-telangiectasia · Biomarkers · Wearable devices · Outcome measures

Introduction

The development of new therapeutics is accelerating for rare and common neurodegenerative diseases with a large unmet medical need [1]. However, currently used tools for determining the efficacy of therapies remain subjective, imprecise, and insensitive. The creation of more sensitive and scalable quantitative motor outcome measures holds the potential to reduce the size, duration, and cost of neurology drug trials.

Ataxia-telangiectasia (A-T) is a rare autosomal recessive neurodegenerative disorder that affects one in every 40,000 to 100,000 children [2]. The neurological manifestation of A-T is characterized by progressive cerebellar atrophy and ataxia, as well as tremor, neuropathy, and extrapyramidal features [3, 4]. Most children with classic A-T do not have obvious motor deficits at birth and walk at a typical age [2, 5]. Gait instability typical of early childhood often fails to resolve with development; however, it is common for motor function to appear stable or mildly improving over the ages of 3 to 7 due to overall gain of gross motor milestones [5]. This masks disease progression and can contribute to delays in diagnosis until hand incoordination, gait imbalance, and other features of the disease worsen [2]. Disease-modifying therapies have the potential to slow or halt the disease process in these early stages [6]; however, it is challenging to

✉ Anoopum S. Gupta
agupta@mgh.harvard.edu

[1] Department of Neurology, Massachusetts General Hospital, Harvard Medical School, 100 Cambridge St, Boston, MA, USA

[2] Stanford University School of Medicine, Stanford, CA, USA

[3] Ataxia Telangiectasia Children's Project, Coconut Creek, FL, USA

prove that the drug is effective in these developmentally dynamic years of child development. Motor impairment progresses during primary school years, and children have difficulty with writing, coloring, and eating, along with increased gait imbalance. By early in the second decade, individuals with A-T begin using a wheelchair [2, 5]. Thus, gait-independent assessment tools are needed to sensitively track disease severity in older children, both for clinical care and to support inclusion in clinical trials.

Clinician-performed ataxia rating scales are currently used for assessments in A-T and other ataxias, including the Brief Ataxia Rating Scale (BARS) [7] and the Scale for the Assessment and Rating of Ataxia (SARA) [8]. Subjectivity and imprecision in these scales necessitate large and long trials, which increase costs, place significant burden on patients, and are a barrier for successful drug development [9, 10]. These scales have additional limitations in pediatric populations; in particular, they are not suitable for children under the age of 4 and demonstrate age dependence in healthy individuals up until 10–12 years of age [11].

Wearable sensors with inertial measurement units (IMU) that contain triaxial accelerometers have been used in A-T and other pediatric ataxias to measure aspects of limb motor impairment during in-clinic administered tasks [12–15]. Multi-sensor IMU systems have been successfully used both inside [16–19] and outside [20] the clinic to quantify gait impairments in different ataxias. These are promising technologies for objective quantification of motor impairment but have limitations in that they are not applicable across all ages and are not designed to accommodate frequent, at-home use in children.

A hallmark characteristic of the ataxia phenotype is that movements are segmented or decomposed into smaller movements [21] or "submovements." Movement segmentation may emerge in part from decreased postural tone and support (e.g., against gravity) during voluntary movements [21], from dyssynchrony of flexor and extensor muscles during coordinated movements [22, 23], and/or from a compensatory strategy to decrease postural disturbances [24]. A recent work demonstrated the utility of quantifying characteristics of wrist submovements in individuals with ataxia during an in-person administered reaching task [14]; however, it is unknown if clinically useful submovement descriptions can be obtained from natural, at-home behavior.

We previously reported that measures of *activity intensity* derived from wrist sensor data collected cross-sectionally at home in 6–18-year-old individuals with A-T were significantly different between A-T and control participants, correlated strongly with ataxia severity, and demonstrated high reliability [25]. Here, we report 1-year longitudinal wrist sensor data in the 6–18-year-old cohort, include new cross-sectional data from children aged 2–6 years old, compare movement features with caregiver-report of function, and develop a novel approach for extracting and characterizing submovements from continuous wrist sensor data. We demonstrate how submovements, in addition to activity intensity measures, are altered in A-T compared with controls, are strongly related to motor severity and function, and are sensitive for detecting disease progression.

Methods

Participants

A total of 31 individuals with A-T and 27 age- and sex-matched healthy siblings and step-siblings ranging in age from 2 to 20 years old participated in the study (see Table 1). Written informed consent and assent were obtained from all participants, and the study was approved by the Partners Healthcare Research Committee Institutional Review Board (No. 2019P002752). Participants were identified in partnership with the Ataxia Telangiectasia Children's Project (A-TCP) and met the following criteria: (i) age between 2 and 20 years, (ii) no history of other neurological or musculoskeletal disorders, (iii) able to tolerate wearing a wrist sensor at home for up to 1 week. Data were collected at two time points. From January to June 2020, 15 children with A-T and 15 controls participated in the study (dataset 1 or DS1). Activity intensity data from DS1 were previously reported [25]. From January to August 2021, 30 children with A-T and 25 controls participated in the study (dataset 2 or DS2). Dataset 2 included 27 individuals who were part of dataset 1 and 28 new participants. Longitudinal wrist sensor data (data from both time points) were available for analysis in 14 children with A-T and 13 controls (LD dataset).

Clinical Assessments and Clinical Data Collection

As described in Khan et al. [25], DS1 included a detailed, in-person neurological exam for each participant with A-T and scoring on BARS, which evaluates gait, speech, oculomotor function, the finger-nose-finger task, and the heel-to-shin task [7]. DS1 also included components of the A-T Neuro Examination Scale Toolkit, [26] in particular for evaluation of hyperkinetic movements.

DS2 included a subset of a caregiver-reported survey called the Caregiver Priorities and Child Health Index of Life with Disabilities (CPCHILD) [27]. Analyses that utilized CPCHILD focused on Sect. 1 and 2, which included 13 questions about personal care (e.g., eating, bathing, toileting, getting dressed) and mobility (e.g., transferring to bed/chair/car, sitting, standing, moving inside and outside). These two sections were included given their relevance to A-T and potential relevance to wrist submovements. This CPCHILD subset score has a range of 0–78, and in contrast to BARS,

Table 1 Participant demographics and clinical characteristics. Participant data is provided separately for Dataset 1, Dataset 2, and the combined Longitudinal Dataset. Nine individuals with A-T are listed as "uncertain" in the A-T phenotype column as they are 6 years old or younger, and it is too early to make a determination

Diagnosis	*N*	Age at start		Sex		Handedness			BARS (0–30)	CPCHILD (0–78)	Wheelchair use (N)	A-T phenotype (*N*)
		Median	Range	M	F	R	L	A				
Dataset 1 (DS1), January-June 2020												
A-T	15	11.0	6.3–18.2	9	6	14	1	0	11.0–25.5	N/A	8	Classic (15)
Control	15	11.0	5.0–16.0	9	6	14	1	0	0	N/A	0	N/A
Dataset 2 (DS2), January–August 2021												
A-T	30	10.8	2.6–20.0	18	12	26	2	2	N/A	20–72	13	Classic (20) Mild (1) Uncertain (9)
Control	25	10.8	2.3–17.2	13	12	21	3	1	N/A	73–78	0	N/A
Longitudinal Data (LD), data from DS1 and DS2												
A-T	14	10.9	6.3–18.2	9	5	13	1	0	11.0–25.5	20–72	7	Classic (14)
Control	13	11.0	5.0–16.0	8	5	12	1	0	0	75–78	0	N/A

*CPCHILD scores reported are for individuals 6–18 years of age

Abbreviations: *A* ambidextrous, *BARS* Brief Ataxia Rating Scale, *CPCHILD* Caregiver Priorities and Child Health Index of Life with Disabilities

lower scores indicate more severe impairment. Individuals 6–18 years old were included in CPCHILD analyses. In-person clinical assessments were not included in DS2 due to the COVID-19 pandemic. Thus, data analysis included cross-sectional analyses of wrist sensor data with respect to clinical assessments and caregiver-reported outcomes, and longitudinal analysis of wrist-sensor data only.

Wearable Sensor Data Collection

The study used the GENEActiv Original actigraphy device (ActivInsights Ltd, Cambridge, UK), which measures tri-axial acceleration at 100 Hz with a MEMS sensor (range: +/−8 g; res: 12bit). Devices were distributed to participants as previously reported [25].

Wearable Sensor Data Processing and Feature Types

Each participant's raw wearable sensor data were partitioned into day and night segments based on clear changes in each child's daily activity level represented in the accelerometer data [25]. To account for differences in the time of day that sensor recording began across participants, day/night segmentation was started at the onset of the first full night of recording. This produced a maximum of 6 consecutive 24-h periods of recording. Data analysis focused on daytime segments. Gravity and high-frequency noise were removed from the acceleration time-series using a sixth-order Butterworth filter with cutoff frequencies of 0.1 and 20 Hz. [28].

Several classes of features were extracted from daytime wrist sensor data for a total of 62 features. These included *total power* in the 0.1–5 Hz frequency range and a set of features based on the distribution of *activity intensity* computed in 1-s time bins, which were previously evaluated cross-sectionally in A-T [25]. These accounted for 8/62 features. The remaining 54/62 features described characteristics of wrist submovements, described in detail below. These included the mean (M) and standard deviation (SD) of submovement distance, peak velocity, and duration (24/62 features), and the mean, standard deviation, and kurtosis (Kr) of shape characteristics of the normalized submovement velocity–time curve (30/62 features).

Activity Index Feature Extraction

Relative scale Activity Index (AI) is a measure of activity intensity derived from tri-axial accelerometry data that correlates with energy expenditure and can differentiate between activity types [29]. The AI metric is based on the variance of acceleration in each of the three axes of motion. AI was computed from the unfiltered acceleration time series for each 1-s period of sensor recording [25]. AI features included the mean, median, mode, and entropy of the AI distribution (excluding periods of inactivity) and the percentage of daytime spent performing low, moderate, and high intensity activities [25].

Submovement Features

Submovements were defined as one-dimensional wrist velocity versus time functions flanked by zero velocity crossings in an analogous way to submovements defined

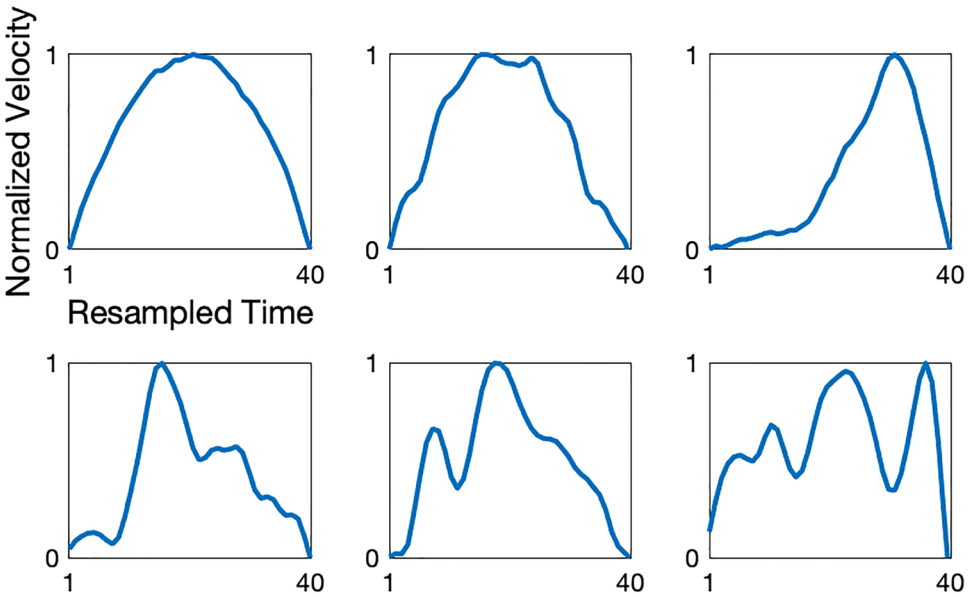

Fig. 1 Examples of normalized submovements from an individual with ataxia-telangiectasia. The x-axis is resampled time so that each submovement is represented by forty time points. The y-axis is velocity, normalized to the range 0–1. Normalized submovements can take on a range of different shapes with varied peak locations and low and high-frequency components

during computer mouse movements [30]. Submovements were extracted from the wrist velocity time series as described in eMethods. Submovements were categorized into four groups based on duration (0.05–0.6 s and 0.6–5 s) and the direction of movement in the plane (primary versus secondary, see eMethods). The mean (M) and standard deviation (SD) of *duration*, *distance*, and *peak velocity* of submovements were computed for each of the four groups, producing 24 features for each individual.

Submovement velocity–time curve (i.e., submovement "shape") characteristics were computed for long duration (0.6–5 s) submovements as described in eMethods. Briefly, submovements were normalized to have velocities ranging 0–1 and were resampled in time to be 40-dimensional (40D) vectors (normalized submovement examples are shown in Fig. 1). Principal component analysis (PCA) was used to identify the top 5 "basis functions" (PC 1–5) that could be used to optimally reconstruct all normalized submovements. The principal component (PC) "scores" for a given submovement are the linear weights on these five principal component vectors in order to reconstruct the submovement. Thus, the magnitude of PC scores represents how much each principal component contributes to the submovement. PC 1 and 2 represented low-frequency characteristics of the velocity–time curve and PC 3–5 represented higher frequency characteristics (Fig. 2). The mean absolute value (M), standard deviation (SD), and kurtosis (Kr) of each principal component score (PC 1–5) for each of the two normalized submovement groups were computed for each individual. In total, this resulted in 30 submovement shape features for each individual.

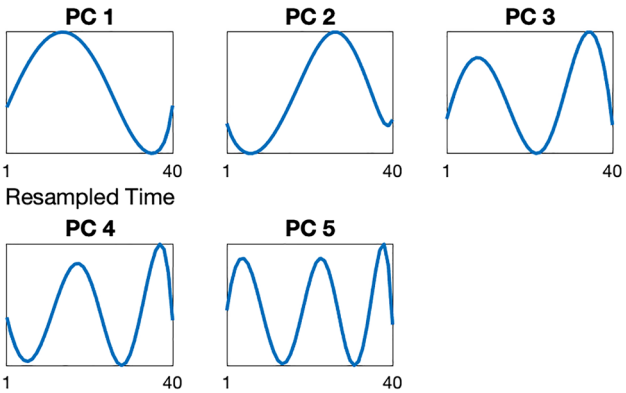

Fig. 2 The top five principal component eigenvectors (PCs), representing basis functions that explain the majority of variance in the submovement velocity versus time curve (i.e., submovement shape). Submovements (see Fig. 1 for examples) can be partially reconstructed by a linear combination of the five principal component vectors shown. Each panel provides a visualization of an eigenvector, with the element values displayed on the y-axis for each dimension of the 40-dimensional vector. PCs 1 and 2 demonstrate a single sine wave cycle with a peak in the first half and second half of the submovement, respectively. PCs 3, 4, and 5 have increasing cycles in half-cycle increments, with 1.5, 2, and 2.5 cycles, respectively

Submovement Feature Grouping

In order to understand and visualize the statistical relationships between the 62 wrist sensor features, features were manually sorted into a smaller set of interpretable feature groups: 3 groups based on activity index and total power, 6 groups based on submovement distance, peak velocity, and duration, and 9 groups based on submovement shape characteristics. For the 3 activity index (AI) groups, AI entropy and

percentage of daytime spent performing low intensity activities were each given their own group. AI mean, median, mode, percentage of daytime spent performing moderate and high intensity activities, and total power were grouped together as they reflect activity intensity in a similar way. The correlation matrix of the 62 features with the 18 feature groups marked is shown in eFigure 3.

Statistical Analyses

All statistical analyses were completed in MATLAB. The Mann–Whitney *U* test was used to determine individual feature and age differences between A-T and control groups, and Cohen's *d* was used to measure effect size. The Wilcoxon signed rank test was used to determine if change in a feature over a 1-year period was different from zero in A-T and control groups. Intraclass correlation coefficients (ICCs) were used to determine the reliability of wrist sensor features over a 1-week recording period (i.e., comparing data from days 1–3 versus days 4–6 from individuals with a full 6 days of data collection): a 2-way mixed effects model was used for evaluation [31]. Absolute value of Pearson correlation coefficients (|*r*|) and *p* values were used to evaluate relationships between wrist sensor features and ataxia rating scales and caregiver reported outcome measures. *p* values less than 0.05 were considered significant. The Benjamini–Hochberg method was used to adjust for multiple comparisons within each of the 18 feature groups of interest [32].

Results

Demographic and clinical information for participants is shown in Table 1. There were no age differences between A-T and control groups in each of the three datasets ($p = 0.27$–0.82). Participants wore the wrist sensor for 5.8 ± 0.7 (M ± SD) full days with a range of 3–6 days.

Wrist Sensor Features Differentiate A-T and Control Participants

Sixteen out of the 18 feature groups contained wrist movement features that were significantly different between A-T and control participants ($p = 2 \times 10^{-2}$-1×10^{-8}, effect

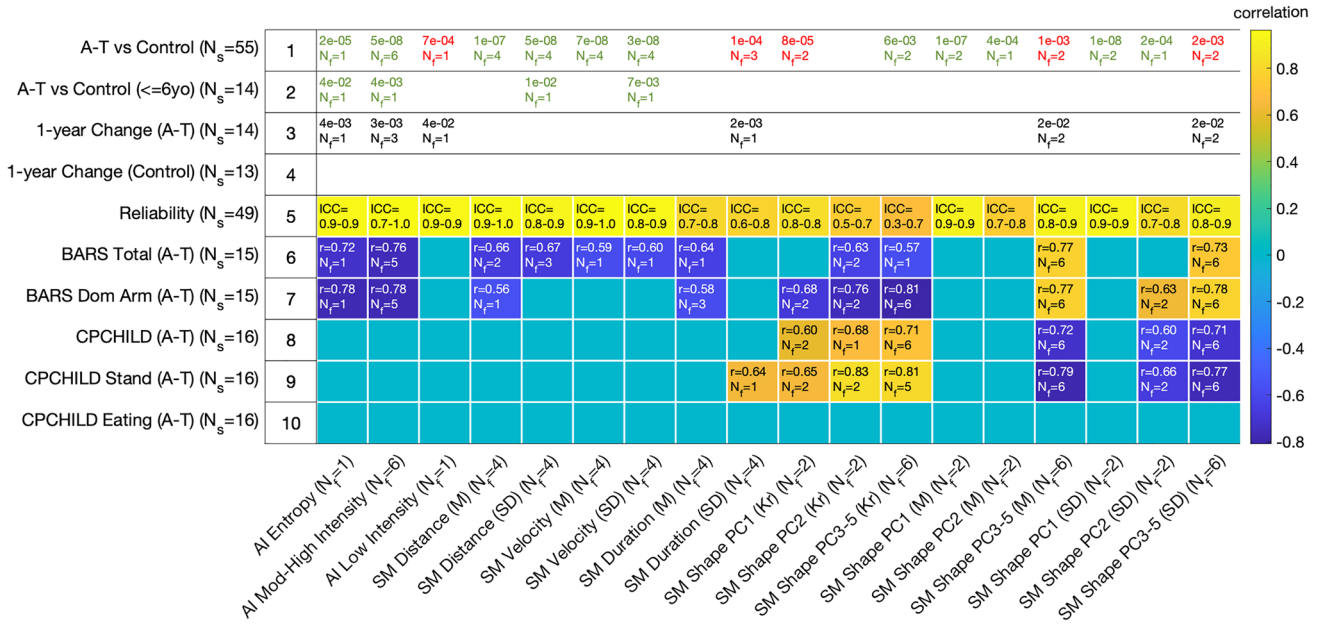

Fig. 3 Relationship between each wrist sensor feature group and key clinical comparisons, including A-T versus control groups (rows 1–2), change over time in the A-T group (row 3) and the control group (row 4), reliability of features for both groups combined (row 5), relationships with the Brief Ataxia Rating Scale (BARS, rows 6–7), and relationships with Caregiver Priorities and Child Health Index of Life with Disabilities (CPCHILD, rows 8–10). Row 4 does not have any text since no features showed statistically significant change in the control group. Rows 1–4 report the number of features (N_f) that are significant within the feature group along with the most significant *p* value. Green text indicates when values are higher in the control group compared with the A-T group, and red text indicates when the value is higher in A-T compared with controls. Rows 5–10 report the number of significant features along with Intraclass Correlation Coefficients (ICC) or maximum absolute value of the Pearson correlation coefficient (*r*). The color of each cell also represents the value of the correlation coefficient. Abbreviations: N_s number of subjects, N_f number of features, *AI* activity intensity, *SM* submovement, *PC* principal component, *M* mean, *SD* standard deviation, *Kr* kurtosis, *ICC* intraclass correlation coefficient, *BARS* Brief Ataxia Rating Scale, *CPCHILD* Caregiver Priorities and Child Health Index of Life with Disabilities

size = 0.6–2.3, Fig. 3, row 1). Four out of these 16 groups had features that remained significantly different when only considering children 6 years old and younger ($p = 0.042$–0.004, effect size = 1.3–2.3, Fig. 3, row 2). Individuals with A-T spent more time performing low intensity movements and less time performing high intensity movements, had shorter and less variable submovement distances, and had slower and less variable submovement peak velocities (Fig. 3, row 1; Fig. 4B,C; eFigure 4, row 1).

A-T submovement velocity versus time profiles (*submovement shapes*) were also significantly different in A-T and control participants. Both low-frequency components (PC 1 and 2) represented a single sine wave cycle, but the peak of the cycle was in the first half of the submovement for PC 1 and was in the second half for PC 2 (Fig. 2). The magnitude and variance of PC 1 scores were larger in controls and highly significant in distinguishing A-T and control participants (Fig. 3, row 1; Fig. 4D). In contrast, A-T submovements had larger and more variable *higher* frequency oscillations. This is reflected by increased mean PC 3 scores in the A-T group—the two significantly different features in the high-frequency group (PC 3–5 M) were PC 3 mean scores in the primary and secondary directions of movement (Fig. 3, row 1). The histogram for PC 3 scores was also less peaked at zero in A-T compared to controls, consistent with larger high-frequency contributions to A-T submovements (Fig. 4F). Thus, submovement velocity–time curves from A-T participants had smaller and less variable low-frequency components, particularly at the beginning of the submovement, and larger and more variable higher frequency components.

Wrist Sensor Features Are Reliable and Capture Disease Progression

For participants in dataset 2 with six full days of data ($N = 49$), the reliability of wrist sensor features was evaluated by comparing features computed from days 1–3 with features obtained from days 4–6. The majority of wrist sensor features showed good to excellent reliability with a median ICC of 0.86 and range of 0.33–0.96 (Fig. 3, row 5).

Data from 27 participants (14 A-T, 13 controls) were collected at two time points separated by 1 year. Features were evaluated for their ability to detect disease progression over the 1-year interval. Features from 6 out of the 18 feature groups demonstrated statistically significant change in the A-T group (Fig. 3, row 3). No features showed significant change in the control group (Fig. 3, row 4). For all features with longitudinal change, the direction of change was congruent with disease progression based on the relationship between the feature and the neurologist-performed ataxia rating scale (BARS). Over the 1-year interval, individuals with A-T had reduced mean activity index (AI) and

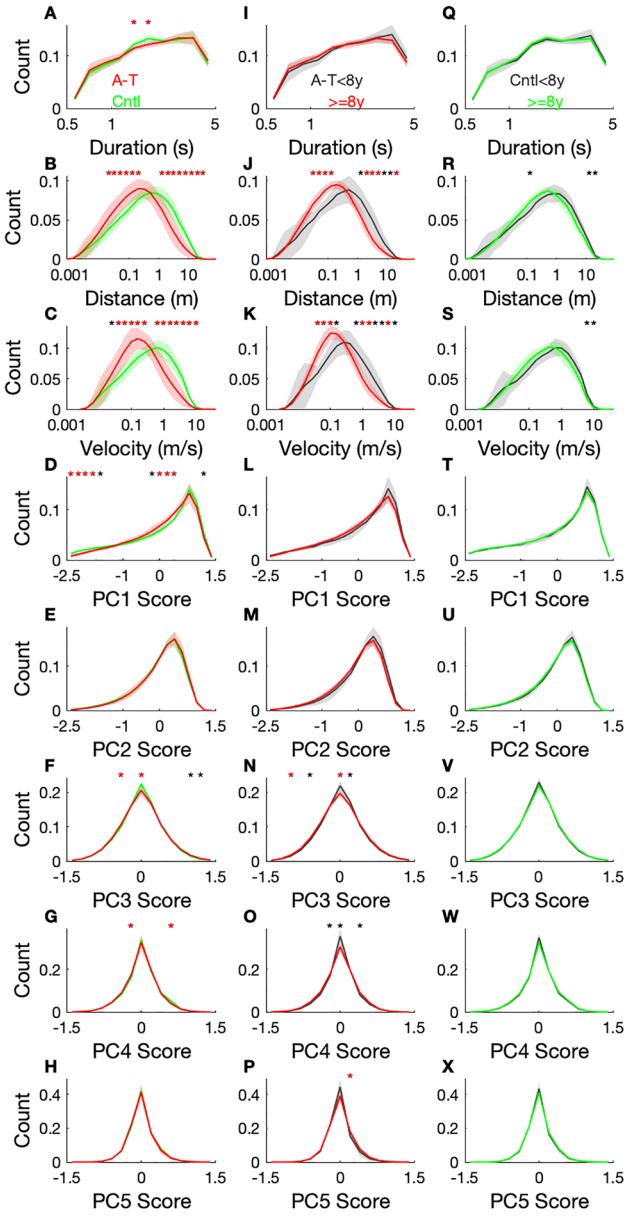

Fig. 4 Normalized histograms of long duration (0.6–5 s) submovement properties for individuals with A-T versus controls (column 1, **A**–**H**), younger versus older individuals with A-T (column 2, **I**–**P**), and younger versus older controls (column 3, **Q**–**X**), for dataset 2 ($N = 55$). Participants with A-T are shown in red and controls in green. The line is the population group mean, and the line width indicates group standard deviation. Duration, distance, and velocity histograms are plotted in log scale. Each histogram bin that is significantly different between groups is marked to indicate the level of significance: $p < 0.001$(*); $p < 0.0001$(red*). Abbreviations: *PC* principal component

decreased AI entropy. There was a trend toward smaller submovement distances, velocities, and durations; however, these did not remain significant after adjustment for multiple comparisons. Submovement shapes had larger high-frequency oscillations (PC 3–5) and more variability

in these high-frequency components (Fig. 3, row 3). These longitudinal observations were further supported by cross-sectional age-group differences in the A-T population: older A-T participants (8 years old and up) had smaller and slower submovements compared with younger A-T participants (Fig. 4J–K). Additionally, older A-T participants had fewer submovements with no high-frequency components, indicated by a smaller histogram peak at PC 3 and PC 4 scores of zero (Fig. 4N–O). These age-group changes were not seen for healthy participants (Fig. 4R–S, V–W), indicating that the changes were largely disease-related rather than age-related changes.

Wrist Sensor Features Correlate with Ataxia Severity and Caregiver-Reported Function

Features from 11 out of 18 feature groups were significantly correlated with BARS total score ($|r|=0.52$–0.77, $p=0.048$–0.0007, Fig. 3, row 6), and features from 10/18 groups were significantly correlated with BARS dominant arm score ($|r|=0.53$–0.81, $p=0.044$–0.0003, Fig. 3, row 7). The wrist movement features that correlated with BARS total and BARS dominant arm were similar to the features that distinguished A-T from control participants and progressed over time in the A-T group. With increasing ataxia severity, the mean and entropy of activity intensity decreased; submovement distances, velocities, and durations decreased and became less variable, and the mean and variance of high-frequency oscillations (PC 3–5) increased (Fig. 3, rows 6–7). Although the magnitude and variance of PC 1 scores were larger in controls and highly significant in distinguishing A-T and control participants, they did not correlate with ataxia severity and did not change over time (Fig. 3, rows 3,6–7). On the other hand, kurtosis of the PC 1–2 and 3–5 distributions, reflecting the amount of probability density outside the central range of the distribution and how heavy-tailed the distributions were, decreased with increasing ataxia severity.

Comparing wrist sensor features with CPCHILD total, standing, and eating scores demonstrated that a subset of wrist sensor features was related to caregiver-reported function (features from 6/14, 7/14, and 0/14 groups, respectively, Fig. 3, rows 8–10). Wrist sensor features had significant relationships with standing ($|r|=0.51$–0.83, $p=0.038$–7×10^{-5}) and overall motor function ($|r|=0.50$–0.72, $p=0.048$–0.0016), whereas there were no significant relationships with eating after adjustment for multiple comparisons. Whereas activity index and submovement distance and peak velocity features were related to ataxia severity and distinguished A-T from controls, they were not significantly correlated with motor function based on CPCHILD. However, variable and increased high-frequency oscillations were significantly correlated with increased motor impairment (Fig. 3, rows 8–9).

Power Law Relationship Between Submovement Velocity and Distance

Prior work has demonstrated a two-thirds power law relationship between submovement velocity and distance during specific motor tasks [33] and a two-thirds power law relationship between curvature and velocity during handwriting and drawing, [34, 35] which may reflect how the motor system plans and optimizes movement [36, 37]. We also observed a strong power law relationship between long duration submovement peak velocity and submovement distance, as indicated by the linear relationship on the log–log 2D histogram (slope: 0.80–0.83, r^2: 0.93; Fig. 5, top row), as well as short duration submovements (slope: 0.69–0.73, r^2: 0.92–0.94; eFigure 5, top row). The power law relationship was similar for A-T and control groups; however, the center of the 2D distribution was shifted toward smaller and slower submovements for the long duration submovements in A-T, consistent with the 1D distance and velocity histograms in Fig. 4B–C.

Discussion

Our results demonstrate that real-life, triaxial accelerometer data from a wrist sensor contain reliable and interpretable information about motor impairment in individuals with ataxia-telangiectasia. Submovement and activity intensity features derived from the wrist sensor data distinguished individuals with A-T from controls, had high reliability, detected disease progression over a 1-year interval, and correlated strongly with ataxia rating scales and caregiver-reported function.

We found that both activity intensity (AI) and submovement feature classes carried information relevant to A-T phenotypes. Consistent with prior work, mean activity intensity and the range of activity intensities were strongly reduced in A-T compared with controls [25]. Additionally, we observed that mean intensity was also significantly reduced in children ≤ 6 years old, and several AI-based features detected disease progression over a 1-year interval. The observed decrease in mean AI and entropy of the AI distribution in A-T participants over time is consistent with the natural history of the disease, which includes slower movements and decreased ability to participate in motor activities over time. While AI-based features correlated with ataxia severity, they did not show statistically significant relationships with caregiver-reported motor function. It is possible that slowing and reducing the intensity of movements assists in the preservation of everyday motor functions, thereby weakening

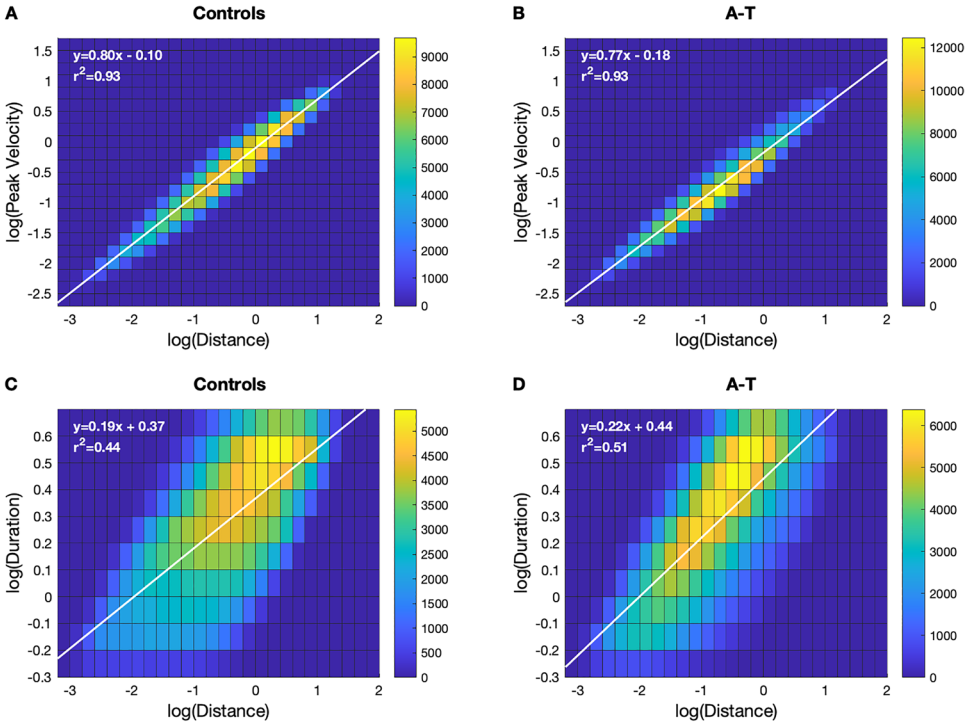

Fig. 5 Two-dimensional, log–log histograms showing the relationships between submovement peak velocity and submovement distance (**A**–**B**) and submovement duration versus distance (**C**–**D**), separately for controls and individuals with A-T for long duration (0.6–5 s) submovements. The linear regression line and equation of each log–log relationship are shown in white. The slope of the line is equivalent to the scaling exponent of the power law relationship between the two variables

the observed relationship between activity intensity features and caregiver-reported function. It is also possible that CPCHILD does not fully capture the motor function changes in A-T, and an A-T-specific caregiver-reported outcome tool is needed.

Submovement kinematic features including peak velocity and distance (mean and variance) were strongly reduced in A-T, and variance of these measures was significantly reduced in the younger age group. Peak velocity, distance, and duration all decreased with increasing ataxia severity but were not significantly correlated with caregiver-reported motor function. This is consistent with the possibility that reductions in movement speed and distance help maintain motor function, resulting in a weaker observed relationship between the variables. Variability in submovement duration significantly decreased over a 1-year interval in A-T participants. Similarly, peak velocity and distance variability trended toward a decrease over time in A-T participants; however, these observations were not significant after adjustment for multiple comparisons. These findings demonstrate that submovement distances, velocities, and durations are decreased in A-T and related to ataxia severity and may become less variable with disease progression.

Submovement shape features captured both low-frequency (PC 1–2) and higher frequency (PC 3–5) oscillations in the velocity–time profile (Fig. 2). The low-frequency component with a velocity peak in the first half of the submovement (PC 1) was much weaker and less variable in A-T compared with controls but did not change with increasing motor severity. On the other hand, the low-frequency component representing a peak in the second half of the submovement (PC 2) became more variable as ataxia severity, and functional impairment increased. Similar to PC 2, the mean and variance of high-frequency (PC 3–5) oscillations increased with worsening ataxia and impaired motor function, and showed progression over a 1-year interval (4/12 features changed in A-T and 0/12 changed in controls, Fig. 3, rows 3–4). The mean and variance of high-frequency oscillations consistently showed moderate to strong relationships with BARS total, BARS arm subscore, CPCHILD total, and CPCHILD standing. They also demonstrated high reliability and detected disease change in A-T participants over a 1-year interval. However, they did not distinguish between A-T and control populations as strongly. This suggests that high-frequency components have different meanings in A-T versus control populations: in controls, high-frequency components may reflect more flexible and complex movement, whereas in A-T they represent decomposed movements which become increasingly segmented with disease progression.

There is evidence that voluntary movements are composed of motor primitives or submovements that are strung together to form motor behaviors [38–40]. Submovements have been observed during ballistic reaching movements [41], slow finger movements [42], rotary wrist movements [43], periodic elliptical drawing [44], and handwriting [33, 34]. Measurements have typically been performed in the laboratory setting using sophisticated equipment

such as motion capture systems or robotic arms to record movements. Our observations of submovement properties during natural movement are consistent with previously reported properties of submovements during motor tasks. Older individuals appear to compensate for greater noise and lower perceptual efficiency by increasing the number of submovements and decreasing the velocity of submovements during accuracy-constrained movement tasks [45]. During the finger-nose-finger reaching task, individuals with different types of cerebellar ataxia were found to have smaller, shorter, and slower submovements, as well as an increased proportion of submovements with more than one velocity peak [14]. Consistent with these observations, but in the context of improving motor function, healthy infants' reaching trajectories become straighter, and movement units decrease in number and increase in duration, with the dominant unit beginning the movement [46]. In stroke survivors during recovery, the number of submovements decreases, and their temporal overlap increases giving rise to smoother trajectories during point-to-point movements [47]. These observations are consistent with the smaller and slower submovements with increased high-frequency oscillations observed in A-T.

It is notable that we observed a bimodal distribution of submovement durations, motivating separation of submovements into short (0.05 – 0.6 s) and long (0.6 – 5 s) duration groups (eFigure 2). The shorter submovements had durations that were largely consistent with those reported in the literature during specific motor tasks. These shorter duration submovements also demonstrated an approximately two-thirds power law relationship between distance and velocity (eFigure 5) that has been previously reported [14, 33]. The longer submovement group included durations that overlapped with prior work, but also included durations that were longer than those reported (mean 0.2–0.44 s, [45] mean 0.2–0.6 s, [46] mean 1.2 s, [47] range 0.05–2.4 s [14]). It is not surprising that there is variation in submovement duration across studies as duration is influenced by motor task parameters [45] and by how submovements are defined and segmented [48]. It is possible that longer duration submovements represent co-articulation or concatenation of movement components and the formation of new movement primitives [39, 49]. If such higher order movement chunks emerge to efficiently represent and control learned movements, one might expect to see these more often during everyday behavior, where well-learned and habitual movements are prevalent. It is also possible that the longer durations we found are in part due to incomplete segmentation of natural behavior submovements. The strong power law relationship between submovement distance and peak velocity ($r^2 = 0.93$) and the reliability of submovement shape features suggest that these long duration submovements are unlikely due to inaccurate segmentation. Furthermore, the strong relationships with ataxia severity and motor function, and consistency with reported changes in older populations, infant development, and stroke recovery, support that longer duration submovements are a meaningful representation of real-life motor behavior.

In summary, the wrist movement changes observed in A-T participants indicate that movements become less intense, with a reduced range of intensities, and submovements become smaller, slower, and less variable in their distances and speeds. The primary low-frequency component, with a peak in the first half of the submovement velocity profile, is reduced and less variable in A-T. These changes suggest that A-T wrist movements during everyday behavior are decomposed into smaller, less powerful, and less flexible submovements. This could reflect a compensatory control mechanism to improve the accuracy and smoothness of movement. These changes could also be in part due to decreased participation in certain types of motor activities. High-frequency components contributed more and were more variable in A-T compared with controls. Increased high-frequency oscillations were strongly related to ataxia severity and impaired motor function and showed progression over a 1-year interval. These larger and more variable high-frequency components may reflect flexor–extensor dyssynergy [50] and/or decomposition of movements into smaller primitives as part of a compensatory strategy [45, 51].

The interpretability, reliability, and sensitivity of movement features extracted from passive wrist sensor data indicate that this technology has potential as an assessment tool and motor outcome measure in A-T clinical trials and clinical care. Importantly, wrist movement characteristics tended to reflect overall ataxia severity and motor function, similarly to or more so than arm-specific ataxia and function subratings. This supports that the motor measurements are ecologically valid and may more closely represent everyday function than measurements from prescribed motor tasks. Since the extraction of submovement and activity intensity features are not dependent on performance of a specific motor task, the same feature types obtained from a sensor worn on the ankle or waist could provide additional information regarding gait, balance, and lower limb function, which is often affected early in A-T. It is also possible that not relying on tasks that are specifically used to assess the ataxia phenotype may enable the current approach to integrate information across the other movement disorders often present in A-T (e.g., chorea), [4, 25] producing a more comprehensive evaluation of the motor state. However, additional research is needed to understand the effects of other movement disorders on submovement and activity intensity properties. The consistency of submovement patterns with studies in other

populations contributes to the validity of the measures and suggests that they could apply to other neurological conditions that affect motor planning and/or execution. As the technology was tested in children as young as 2 years old as well as in individuals who were wheelchair bound, it has potential for application across a wide age range and spectrum of disease severity. Finally, the use of a low-cost, low-burden sensor that is ubiquitous in smartwatches could support participation in neurological care and research for individuals regardless of geography and socioeconomic status.

There were several limitations of the study. First, the sample size of the study was relatively small, and the population contained a wide range of disease severity and age. A larger population of participants in the youngest age group would support analysis of wrist movement patterns during periods of rapid motor development and enable a detailed characterization of the age dependence of wrist sensor features. A-T participants were recruited from across the USA to obtain as representative a sample as possible in this rare disease population. Future research is needed to build upon these findings in larger and more homogeneous neurological disease populations. BARS, similar to other ataxia rating scales, is age dependent up to approximately 11 years of age [11]. Thus it is possible that motor immaturity contributed in part to the observed relationships between wrist sensor features and BARS ratings. Natural wrist movements in the real world are generated as part of a very large range of motor behaviors. Our analysis of wrist submovements ignores different types of behaviors and treats them as a single group. Caution is needed in comparing submovement properties during natural behavior with submovement properties during well-controlled motor tasks due to important differences in behavioral context as well as differences in how submovements are identified.

Supplementary Information The online version contains supplementary material available at https://doi.org/10.1007/s12311-022-01385-5.

Acknowledgements The authors thank Rachelle Gupta and Siddharth Patel for helpful comments on the manuscript. The authors would also like to thank the patients and families who collaborated with us on this project.

Author Contribution All authors contributed to the study conception and design. ACL, NCK, SR, and JKT contributed to the acquisition of data. ASG performed the data analysis and wrote the first draft of the manuscript. All authors revised the manuscript for intellectual content.

Funding ASG is a consultant for Biogen Inc., Triplet Therapeutics, and Remix Therapeutics and is funded by NINDS R01 NS117826, the Massachusetts Life Sciences Center, Biogen Inc., the Ataxia-Telangiectasia Children's Project, and the University of Pennsylvania Orphan Disease Center. ACL, NCK, SR, and JKT have no disclosures to report.

Data Availability All data included in this study will be shared by request from any qualified investigator.

Declarations

Ethics Approval Written informed consent and assent were obtained from all participants prior to participation, and the study was approved by the Partners Healthcare Research Committee Institutional Review Board (No. 2019P002752).

Conflict of Interest The authors declare no competing interests.

References

1. Cavazzoni, P. The Path forward: advancing treatments and cures for neurodegenerative diseases. https://www.fda.gov/news-events/congressional-testimony/path-forward-advancing-treatments-and-cures-neurodegenerative-diseases-07292021#footnote1Footnote reference is out of range._sde0aq9 (2021).
2. Rothblum-Oviatt C, et al. Ataxia telangiectasia: a review. Orphanet J Rare Dis. 2016;11:1–21.
3. Lavin MF, Gueven N, Bottle S, Gatti RA. Current and potential therapeutic strategies for the treatment of ataxia-telangiectasia. Br Med Bull. 2007;81–82:129–47.
4. Nissenkorn, A. & Ben-Zeev, B. *ataxia telangiectasia*. vol. 132 (Elsevier B.V., 2015).
5. Crawford TO. Ataxia telangiectasia. Semin Pediatr Neurol. 1998;5:287–94.
6. Bennett CF, Krainer AR, Cleveland DW. Antisense oligonucleotide therapies for neurodegenerative diseases. Annu Rev Neurosci. 2019;42:385–406.
7. Schmahmann JD, Gardner R, MacMore J, Vangel MG. Development of a brief ataxia rating scale (BARS) based on a modified form of the ICARS. Mov Disord. 2009;24:1820–8.
8. Schmitz-Hübsch T, et al. Scale for the assessment and rating of ataxia: development of a new clinical scale. Neurology. 2006;66:1717–20.
9. Rummey C, Kichula E, Lynch DR. Clinical trial design for Friedreich ataxia—where are we now and what do we need? Expert Opin Orphan Drugs. 2018;6:219–30.
10. Brooker SM, Edamakanti CR, Akasha SM, Kuo SH, Opal P. Spinocerebellar ataxia clinical trials: opportunities and challenges. Annals of Clinical and Translational Neurology. 2021;8:1543–56.
11. Brandsma R, et al. Ataxia rating scales are age-dependent in healthy children. Dev Med Child Neurol. 2014;56:556–63.
12. Shaikh AG, Zee DS, Mandir AS, Lederman HM, Crawford TO. Disorders of upper limb movements in ataxia- telangiectasia. 2013;8:4–9.
13. Martinez-Manzanera O, et al. Instrumented finger-to-nose test classification in children with ataxia or developmental coordination disorder and controls. Clin Biomech. 2018;60:51–9.
14. Oubre B, et al. Decomposition of reaching movements enables detection and measurement of ataxia. Cerebellum. 2021. https://doi.org/10.1007/s12311-021-01247-6.
15. Knudson, K. C. & Gupta, A. S. Assessing cerebellar disorders with wearable inertial sensor data using time-frequency and autoregressive hidden MARKOV model Approaches. (2021).
16. LeMoyne, R. *et al.* Wearable body and wireless inertial sensors for machine learning classification of gait for people with Friedreich's ataxia. *BSN 2016—13th Annual Body Sensor Networks Conference* 147–151 (2016).

17. Hickey A, et al. Validity of a wearable accelerometer to quantify gait in spinocerebellar ataxia type 6. Physiol Meas. 2016;37:N105–17.
18. Terayama K, Sakakibara R, Ogawa A. Wearable gait sensors to measure ataxia due to spinocerebellar degeneration. Neurol Clin Neurosci. 2018;6:9–12.
19. Shah VV, et al. Gait variability in spinocerebellar ataxia assessed using wearable inertial sensors. Mov Disord. 2021. https://doi.org/10.1002/mds.28740.
20. Ilg W, et al. Real-life gait assessment in degenerative cerebellar ataxia: toward ecologically valid biomarkers. Neurology. 2020;95:e1199–210.
21. Holmes, G. The Cerebellum of Man. (1939).
22. Babinski J. Sur le rôle du cervelet dans les actes volitionnels nécessitant une succession rapide de mouvements (diadococinésie). Rev Neurol. 1902;10:1013–5.
23. Vilis T, Hore J. Effects of changes in mechanical state of limb on cerebellar intention tremor. J Neurophysiol. 1977;40:1214–24.
24. Morton SM, Bastian AJ. Relative contributions of balance and voluntary leg-coordination deficits to cerebellar gait ataxia. J Neurophysiol. 2003;89:1844–56.
25. Khan NC, Pandey V, Gajos KZ, Gupta AS. Free-living motor activity monitoring in ataxia-telangiectasia. Cerebellum. 2021. https://doi.org/10.1007/s12311-021-01306-y.
26. Jackson TJ, et al. Longitudinal analysis of the neurological features of ataxia-telangiectasia. Dev Med Child Neurol. 2016;58:690–7.
27. Narayanan UG, et al. Initial development and validation of the Caregiver Priorities and Child Health Index of Life with Disabilities (CPCHILD). Dev Med Child Neurol. 2006;48:804–12.
28. Bouten CV, Koekkoek KT, Verduin M, Kodde R, Janssen JD. A triaxial accelerometer and portable data processing unit for the assessment of daily physical activity. IEEE Trans Biomed Eng. 1997;44:136–47.
29. Bai J, et al. An activity index for raw accelerometry data and its comparison with other activity metrics. PLoS ONE. 2016;11:1–14.
30. Walker N, Meyer DE, Smelcer JB. Spatial and temporal characteristics of rapid cursor-positioning movements with electromechanical mice in human-computer interaction. Hum Factors. 1993;35:431–58.
31. Shrout PE, Fleiss JL. Intraclass correlations: Uses in assessing rater reliability. Psychol Bull. 1979;86:420–8.
32. Benjamini Y, Hochberg Y. Controlling the false discovery rate: a practical and powerful approach to multiple testing. J R Stat Soc. 1995;57:289–300.
33. Miranda, J.G.V., Daneault, JF., Vergara-Diaz, G. et al. Complex Upper-Limb Movements Are Generated by Combining Motor Primitives that Scale with the Movement Size. Sci Rep 8, 12918 (2018). https://doi.org/10.1038/s41598-018-29470-y
34. Viviani P, Terzuolo C. Trajectory determines movement dynamics. Neuroscience. 1982;7:431–7.
35. Lacquaniti F, Terzuolo C, Viviani P. The law relating the kinematic and figural aspects of drawing movements. Acta Psychol. 1983;54:115–30.
36. Viviani P, Flash T. Minimum-jerk, two-thirds power law, and isochrony: converging approaches to movement planning. J Exp Psychol Hum Percept Perform. 1995;21:32–53.
37. Richardson MJE, Flash T. Comparing smooth arm movements with the two-thirds power law and the related segmented-control hypothesis. J Neurosci. 2002;22:8201–11.
38. Viviani P. Do units of motor action really exist? Experimental Brain Research Series. 1986;15:201–16.
39. Flash T, Hochner B. Motor primitives in vertebrates and invertebrates. Curr Opin Neurobiol. 2005;15:660–6.
40. Hogan N, Sternad D. Dynamic primitives of motor behavior. Biol Cybern. 2012;106:727–39.
41. Flash T, Hogan N. The coordination of arm movements: an experimentally confirmed mathematical model. J Neurosci. 1985;5:1688–703.
42. Vallbo AB, Wessberg J. Organization of motor output in slow finger movements in man. J Physiol. 1993;469:673–91.
43. Crossman ER, Goodeve PJ. Feedback control of hand-movement and Fitts' Law. Q J Exp Psychol A. 1983;35:251–78.
44. Viviani P, Cenzato M. Segmentation and coupling in complex movements. J Exp Psychol Hum Percept Perform. 1985;11:828–45.
45. Walker, N., Philbin, D. A. & Fisk, A. D. Age-related differences in movement control: adjusting submovement structure to optimize performance. *J. Gerontol. B Psychol. Sci. Soc. Sci.* **52B**, P40–P53 (1997).
46. von Hofsten C. Structuring of early reaching movements: a longitudinal study. J Mot Behav. 1991;23:280–92.
47. Rohrer B, et al. Submovements grow larger, fewer, and more blended during stroke recovery. Mot Control. 2004;8:472–83.
48. Rohrer B, Hogan N. Avoiding spurious submovement decompositions: a globally optimal algorithm. Biol Cybern. 2003;89:190–9.
49. Sosnik R, Hauptmann B, Karni A, Flash T. When practice leads to co-articulation: the evolution of geometrically defined movement primitives. Exp Brain Res. 2004;156:422–38.
50. Hallett M, Shahani BT, Young RR. EMG analysis of patients with cerebellar deficits. J Neurol Neurosurg Psychiatry. 1975;38:1163–9.
51. Bastian AJ, Martin TA, Keating JG, Thach WT. Cerebellar ataxia: abnormal control of interaction torques across multiple joints. J Neurophysiol. 1996;76:492–509.